Reconsidering the Origins of Forsbergh Birefringence Patterns

A. Schilling[1], A. Kumar[1], R. G. P. McQuaid[1], A. M. Glazer[2,3], P. A. Thomas[3], J. M. Gregg[1*]

[1]*Centre for Nanostructured Media, School of Mathematics and Physics, Queen's University Belfast, Belfast, BT7 1NN, U.K.*

[2]*Clarendon Laboratory, Parks Road, Oxford, OX1 3PU, U.K.*

[3]*Department of Physics, University of Warwick, Gibbet Hill Road, Coventry, CV4 7AL, U.K.*

*corresponding author email: m.gregg@qub.ac.uk

Abstract

In 1949, P. W. Forsbergh Jr. reported spontaneous spatial ordering in the birefringence patterns seen in flux-grown $BaTiO_3$ crystals [1], under the transmission polarized light microscope [2]. Stunningly regular square-net arrays were often only found within a narrow temperature window and could be induced on both heating and cooling, suggesting genuine thermodynamic stability. At the time, Forsbergh rationalized the patterns to have resulted from the impingement of ferroelastic domains, creating a complex tessellation of variously shaped domain packets. However, evidence for the intricate microstructural arrangement proposed by Forsbergh has never been found. Moreover, no robust thermodynamic argument has been presented to explain the narrow region of thermal stability, its occurrence just below the Curie Temperature and the apparent increase in entropy associated with the loss of the Forsbergh pattern on cooling. As a result, despite decades of research on ferroelectrics, this ordering phenomenon and its thermodynamic origin have remained a mystery. In this paper, we re-examine the microstructure of flux-grown $BaTiO_3$ crystals, which show Forsbergh birefringence patterns. Given an absence of any obvious arrays of domain polyhedra, or even regular shapes of domain packets, we suggest an alternative origin for the Forsbergh pattern, in which sheets of orthogonally oriented ferroelastic stripe domains simply overlay one another. We show explicitly that the Forsbergh birefringence pattern occurs if the periodicity of the stripe domains is above a critical value. Moreover, by considering well-established semiempirical models, we show that the significant domain coarsening needed to generate the Forsbergh birefringence is fully expected in a finite window below the Curie Temperature. We hence present a much more straightforward rationalization of the Forsbergh pattern than that originally proposed, in which exotic thermodynamic arguments are unnecessary.

The spontaneous formation of periodic arrays, that go beyond ordered atomic arrangements in conventional crystals, is both visually arresting and scientifically compelling; hexagonal arrays of flux quanta (and associated supercurrent vortices) in Type II superconductors (Abrikosov vortex arrays) [3-5], topologically complex magnetic dipole skyrmion arrays [6-9] and static charge density wave structures [10,11], for example, all generate very strong research interest. The underlying physics responsible for the appearance of these ordered states is fascinating and the potential discovery of unique properties, that novel periodic arrays might possess, demands thorough investigation.

In ferroelectrics, the formation of ordered arrays of dipole vortices has been predicted using atomistic simulations in nanoscale geometries [12, 13]. Experimentally, individual flux-closure objects, ordered arrangements of flux-closed states into chains, and genuine dipole vortex arrays have been seen [14-22]. Examination of their dynamics of formation [23] and the functional properties of these systems are currently ongoing [24]. Despite this recent flurry of research activity, the suggestion that dipole groups in ferroelectrics might spontaneously form into periodic arrays is not new. Over 65 years ago Forsbergh [2], Matthias and von Hippel [25] and later Nakamura [26-28], Lambert [29] and coworkers observed that domains in flux-grown $BaTiO_3$ generated striking square-net birefringence patterns, just below the Curie Temperature (T_C). The phenomenon is illustrated in figure 1, which has been produced by an automatic polarizing microscope system (METRIPOL) [30]. This uses a rotating polarizer and a circular analyzer for which the intensity transmitted is given by

$$I = \frac{I_0}{2}[1 - 2\sin(2\alpha - 2\phi)\sin\delta] \qquad (1)$$

where I_0 is the transmitted light after absorption through the specimen and δ is the phase shift induced and is related to the birefringence by

$$\delta = \frac{2\pi}{\lambda}(n_1 - n_2)d = \frac{2\pi\Delta nd}{\lambda} \qquad (2)$$

ϕ is the orientation of a major axis of the optical indicatrix and α is the angle of rotation of the polarizer at any time; d is the sample thickness. Images are collected on a CCD typically at 5 or 10 values of α. By refining the intensity at each pixel in the image it is possible to separate out the three quantities I_0, $|\sin\delta|$ and ϕ, which are then used to create new false-colour images. The images seen in figure 1 are from a film showing the change in orientation ϕ and in $|\sin\delta|$ with temperature (the complete videos can be downloaded from the supplementary information section).

In his original work, Forsbergh noted that the regular birefringent patterns only occurred when orthogonally oriented sets of 90° a-c ferroelectric-ferroelastic domains met.

He supposed that the impingement of these sets induced the formation of a complex array of pyramids containing a-a stripe domains, pyramids of a single domain variant and tetrahedra containing a-c stripe domains. We note that in later work, Lambert *et al.* [29] suggested that a much less convoluted domain pattern could form when two orthogonal a-c packets intersected. However, in both approaches, square net birefringence was directly linked to an ordered array of domain polyhedra and in neither case was an explanation given for the periodic birefringence often only occurring within a distinct temperature range below T_c. We directly examined the domain patterns evident at room temperature near the surface of a thin flux-grown crystal, displaying a Forsbergh birefringence pattern with a period of ~50μm, using piezoresponse force microscopy (PFM) and cross-sectional scanning transmission electron microscopy (STEM). As can be seen in figure 2, packets of 90^o ferroelectric-ferroelastic domains are evident, but their distribution is irregular and there is no indication of the kinds of well-defined polyhedral shapes suggested by Forsbergh. There are several interpretations for this finding: firstly, that the Forsbergh birefringence pattern is not related to tessellated polyhedra in the manner originally postulated; secondly, that the polyhedra are still present, but buried beneath a skin layer with a different domain structure [31, 32]; thirdly, that the polyhedra only develop within the temperature range below T_C in which the Forsbergh pattern can be seen and are then destroyed on further cooling to room temperature. We attempted to examine the domains at elevated temperatures using PFM, but the signal to noise ratio became unfavourable. Nevertheless, we found no suggestion of the development of strongly ordered polyhedra at the surface just below T_C.

Given the complexity of the polyhedral microstructure suggested by Forsbergh and the lack of direct evidence for it, other potential origins for the birefringence square-net array need to be considered. Our optical observations confirmed the strong association between the coincidence of orthogonal sets of a-c domains and the existence of the Forsbergh birefringence pattern (figure 3a). However, we recognize that in transmission microscopy it is not always trivial to tell differences in the heights at which the imaged orthogonal domain sets occur. Therefore, rather than make conjectures about the manner in which a-c domain sets might impinge [2,29], we here consider the birefringence that can be generated when two identical sheets of orthogonal a-c domains are stacked on top of each other (figure 3b).

Below T_C, $BaTiO_3$ belongs to the space group P4mm and has an associated negative uniaxial optical indicatrix. When polarized light propagates perpendicular to a single slab of a-c domains, the total retardation at each point is therefore given by the total

thickness of the a-domains locally perpendicular to the slab multiplied by the difference between the refractive indices parallel to the a and c axes. Perpendicularly polarized light components passing through the c-domains are parallel to the optic axis and hence do not experience any relative retardation. If the domain periodicity (ω) is relatively fine in relation to the thickness of the slab (d), then the overall retardation shows no spatial variation. However, if the domain period is sufficiently coarse that the ω / d ratio exceeds a critical value of $\sqrt{2}/2$, then spatial modulation in retardation will start to become evident and will locally reach a maximum value of $d.(n_1\text{-}n_3)$ (where n_1 and n_3 are the refractive indices along the a and c crystallographic directions in $BaTiO_3$) once a second critical ω / d ratio of $\sqrt{2}$ is reached and exceeded (figure 4a).

For two identical, orthogonally oriented, slabs of a-c domains, stacked one above the other, the overall retardation in two dimensions (*x,y*) is given by:

$$\Delta = (t_1 n_1 + t_2 n_3) - (t_1 n_3 + t_2 n_1) \qquad (3)$$

where t_1 and t_2 are the total thicknesses of a-domains perpendicular to the slab surfaces in slab 1 and 2 respectively, and are both functions of *x* and *y*. For the specific condition that $\omega / d = \sqrt{2}$, the retardation has been calculated explicitly and the resultant form of the birefringence pattern is shown in figure 4b. The similarity to the Forsbergh birefringence pattern is self-evident. Even if the two slabs are not of identical thickness, square-net birefringence patterns still develop as shown by the relative retardation pattern generated in figure 4c. Here one slab is kept the same as that considered above (with a ω / d ratio of $\sqrt{2}$), while the thickness of the second overlaying slab has been increased by a factor of 1.5. The change in thickness was considered to also be associated with a change in the domain period (the domain period increases as the slab thickness increases), consistent with the Landau-Kittel scaling law discussed below. While the pattern generated (figure 4c) is clearly different from that shown in figure 4b, square-net features are still evident; indeed, there are areas in the images shown in Forsbergh's original article [2] that are strongly reminiscent of those in figure 4c.

We should now address reasons why a birefringence pattern generated in this way might not be seen at room temperature, but may be seen just below T_C: the Landau-Kittel scaling law for stripe domains generates the condition that, under equilibrium

$$\omega^2 = \frac{\gamma}{U} d = kd \qquad (4)$$

where γ is a domain wall energy density term, U is an energy term associated with the order parameter within a domain being expressed uniformly (strain, polarization or

magnetization in the same sense, for example), k is equal to γ/U and d is traditionally taken to be the crystal thickness. In previous research [33], on modern commercially grown $BaTiO_3$ crystals (top-seeded), we have seen that when packets of domains are evident in the microstructure, the local dimensions of the packets define the thicknesses that determine the equilibrium periodicity of the stripe domains they contain; the overall crystal dimensions are not of primary importance. Figure 5a, for example, shows a Scanning Transmission Electron Microscopy (STEM) image of a $BaTiO_3$ nanocolumn (taken at room temperature), patterned from a bulk single crystal as described in [33]. The periodicity of the ferroelastic domains responsible for the stripe contrast within these columns can be seen to vary. It is approximately constant, when the domain packet size is defined by the width of the column, but decreases as the domain packet size is progressively constrained into the triangular points, formed at junctions between packets of stripe domains. By taking measurements of the individual domain period of pairs of domains (an effective ω) as a function of the local packet width at each point (an effective dimension d), reasonable adherence to Landau-Kittel scaling can be seen (figure 5b). Thus, in our model, d is taken to refer to the thickness of each of the two slabs of a-c stripe domains and not the overall thickness of the crystal. As mentioned above, for contrast associated with the Forsbergh birefringence pattern to even begin to emerge, $\omega/d \geq \sqrt{2}/2$. Using equation (4), this condition can be re-expressed in terms of d only as follows:

$$\frac{\omega^2}{d^2} \geq \frac{1}{2} \text{ and hence } \frac{k}{d} \geq \frac{1}{2}$$
$$\therefore d \leq 2k \qquad (5)$$

For thin free-standing $BaTiO_3$ sheets cut from recently grown commercial single crystals (top seeded), Schilling *et al.* have already mapped the periodicity of 90° stripe domains as a function of thickness [34] and confirmed adherence to Landau-Kittel scaling, with k ~ 45nm. Similar data from flux-grown samples is unfortunately not available. However, if similar parameters transfer to flux-grown $BaTiO_3$, this implies that the effective thickness of individual a-c slabs would have to be below ~100nm for stripe domains to be sufficiently coarse (relative to the slab thickness) for a periodic birefringent pattern to even begin to emerge under equilibrium conditions at room temperature. This scale of microstructure may be too fine to occur in most circumstances.

However, using temperature-variable PFM on the same batch of crystals used in Schilling *et al.*'s work [34], McGilly *et al.* [35] have already directly observed that ferroelastic stripe domains in $BaTiO_3$ significantly coarsen within a few degrees of T_C. In

addition, they have rationalized the coarsening phenomenon by adapting a number of established semiempirical models to obtain the expression:

$$\omega(T) = c\left[\frac{\gamma(T)d}{E(T)s(T)^2}\right]^{1/2} \quad (6)$$

where the domain period (ω) is now a function of temperature (T), as is the domain wall energy density (γ), Young's modulus (E) and spontaneous strain (s); c is a temperature-independent constant. The form of this expression is valid for any ferroelectric system. Using the same literature sources [36-38] for $\gamma(T)$, $E(T)$ and $s(T)$ as used by McGilly *et al.*, we have plotted the behaviour of ω/d as a function of temperature implied by equation (6) in figure 5c. Importantly, studies [36] and [38] involve either direct measurements on flux-grown crystals, or the use of data taken from prior measurements on flux-grown crystals and so are particularly relevant for this discussion. Reference [37] involves the study of ceramic $BaTiO_3$, but when the behavior of the Young's Modulus around and below T_C taken from [37] is extrapolated to room temperature, it approximates well to the values determined at room temperature specifically for flux-grown single crystals [39, 40]. The form of the function shown in figure 5c makes it clear that the two critical values associated with observable periodic birefringence development should only occur close to T_C. It should be noted that, as the dimensions of the domain packets decrease, the thermal stability of the Forsbergh pattern increases. In principle, this nicely rationalizes the existence of the narrow temperature window, just below T_C, in which the Forsbergh birefringence is observed.

Unfortunately, direct use of data obtained, interpolated and extrapolated from references [36-38] predicts a temperature window which is dramatically narrower than that associated with the images in figure 1, where stable Forsbergh patterns exist between 111°C and the Curie Temperature (measured through birefringence to be ~120°C). This would be equivalent to the onset of square-net birefringence at T/T_C of ~ 0.98 compared to the ~0.9975 associated with figure 5c. We note, however, that the behavior of the spontaneous strain, measured using X-ray diffraction by Walker *et al.* [41], on the same crystals as those illustrated in figure 1, shows a dramatic collapse at 111°C. Equation (6) shows that the domain periodicity is strongly dependent on spontaneous strain and so the temperature dependence of ω/d was recalculated using the Walker *et al.* data, as opposed to that from Megaw [38]. As can be seen, in figure 5d, this dramatically expands the thermal window in which Forsbergh patterns should be visible: in this case to T/T_C ~0.98, for a slab thicknesses around 50μm. This T/T_C value matches experiment extremely well, as the sharp anomaly in ω/d seen in figure 5d is a direct result of the

collapse in spontaneous strain observed. The slab thickness of 50μm implies an overall crystal thickness of 100μm, which is somewhat thinner than the crystals examined. However, in calculating the values of $^{\omega}/_{d}$ in figure 5d, we have assumed that the strain measured by Walker *et al.* between 111°C and 120°C is entirely due to the spontaneous strain in the system. This is erroneous, as Walker *et al.* explicitly state that most of this observed strain within this temperature window is not due to spontaneous strain, but is rather residual strain in the crystal; our calculated values of $^{\omega}/_{d}$ for each slab thickness are therefore underestimated in the region $0.98<T/T_C<1$. Unfortunately, Walker *et al.* could not explicitly determine the relative contribution of the spontaneous strain in this temperature window and so we are forced to accept that the crystal thickness of 100μm is a lower limit estimate and that the actual maximum thickness at which Forsbergh patterns may be seen should be significantly higher.

In summary, we have re-evaluated the potential origins for the spontaneously occurring self-ordered pattern of birefringence that has been known to occur in flux-grown $BaTiO_3$ crystals for over 65 years. Despite the obvious complexity of the original explanation, suggested by Forsbergh, few alternative models have been forthcoming to date. Rather, it has been widely accepted for decades that transient complex arrays of tessellating polyhedra spontaneously form just below T_C, because of the impingement of orthogonal a-c domain sets, and then disappear on further cooling. Since microstructural investigations, of regions of crystal in which Forsbergh birefringence occurs, do not show direct evidence for highly ordered arrangements of specific domain polyhedra, an alternative and simpler explanation has been considered, in which orthogonally oriented slabs of a-c domains are stacked one above the other. We have shown that this arrangement can readily generate the Forsbergh birefringence pattern, provided the periodicity of the a-c domains is sufficiently coarse in relation to the thickness of the slabs. At room temperature and under the equilibrium scaling laws developed by Kittel and by Landau and Lifshitz, Forsbergh birefringence should only be evident if the slabs are thinner than ~100nm. However, on heating, we show that this condition is dramatically relaxed and, close to T_C, domain coarsening caused by reductions in spontaneous strain, should result in a distinct window in which the Forsbergh birefringence array would be observed. The size of this thermal window increases dramatically when the spontaneous strain collapse measured by Walker *et al.* is explicitly considered. The simplicity of the required microstructure and the associated straightforward explanation for a region of thermal stability for the square-net birefringence below T_C make our stacked slab model an attractive alternative explanation to that given by Forsbergh.

References:

[1] H. Blattner, B. Matthias, and W. Mertz, Helv. Phys. Acta, **20**, 225 (1947**)**; J. P. Remeika, J. Am. Chem. Soc., **76**, 940 (1954).

[2] P. W. Forsbergh, Jr., Phys. Rev., **76**, 1187 (1949).

[3] H. F. Hess, R. B. Robinson, R. C. Dynes, J. M. Valles, Jr., and J. V. Waszczak, Phys. Rev. Lett., **62**, 214 (1989).

[4] U. Essmann and H. Trauble, Phys. Lett., **24A**, 526 (1967).

[5] P. L. Gammel, D. J. Bishop, G. J. Dolan, J. R. Kwo, C. A. Murray, L. F. Schneemeyer, and J. V. Waszczak, Phys. Rev. Lett., **59**, 2592 (1987).

[6] S. Mühlbauer, B. Binz, F. Jonietz, C. Pfleiderer, A. Rosch, A. Neubauer, R. Georgii, P. Böni, Science, **323**, 915 (2009).

[7] X. Z. Yu, Y. Onose, N. Kanazawa, J. H. Park, J. H. Han, Y. Matsui, N. Nagaosa and Y. Tokura, Nature, **465**, 901 (2010).

[8] Christian Pfleiderer, Nature Physics, **7**, 673 (2011).

[9] A. Neubauer, C. Pfleiderer, B. Binz, A. Rosch, R. Ritz, P.G. Niklowitz and P. Boni, Phys. Rev. Lett., **102**, 186602 (2009).

[10] A. Soumyanarayanan, M. M. Yee, Y. He, J. van Wezel, D. J. Rahn, K. Rossnagel, E. W. Hudson, M. R. Norman, J. E. Hoffman, PNAS, **110**, 1623 (2013).

[11] K. C. Rahnejat, C. A. Howard, N. E. Shuttleworth, S. R. Schofield, K. Iwaya, C. F. Hirjibehedin, Ch. Renner, G. Aeppli, and M. Ellerby, Nat. Commun., **2**, 558 (2011).

[12] I. I. Naumov, L. Bellaiche and H. Fu, Nature, **432**, 737 (2004).

[13] H. Fu and L. Bellaiche, Phys. Rev. Lett., **91**, 25760 (2003).

[14] Y. Ivry, D. P. Chu, J. F. Scott and C. Durkan, Phys. Rev. Lett., **104**, 207602 (2010).

[15] L. J. McGilly and J. M. Gregg, Nano Lett., **11**, 4490 (2011).

[16] R. G. P. McQuaid, L. J. McGilly, P. Sharma, A. Gruverman and J. M. Gregg, Nat. Commun., **2**, 404 (2011).

[17] N. Balke, S. Choudhury, S. Jesse, M. Huijben, Y. H. Chu, A. P. Baddorf, L. Q. Chen, R. Ramesh and S. V. Kalinin, Nat. Nanotechnol., **4**, 868 (2009).

[18] R. K. Vasudevan, Y.-C Chen, H.-H. Tai, N. Balke, P. Wu, S. Bhattacharya, L. Q. Chen, Y.-H. Chu, I.-N. Lin, S. V. Kalinin and V. Nagarajan, ACS Nano, **5**, 879 (2011).

[19] L. J. McGilly, A. Schilling and J. M. Gregg, Nano Lett., **10**, 4200 (2010).

[20] L-W. Chang, V. Nagarajan, J. F. Scott and J. M. Gregg, Nano Lett., **13**, 2553 (2013).

[21] Y. L. Tang, Y. L. Zhu, X. L. Ma, A. Y. Borisevich, A. N. Morozovska, E. A. Eliseev, W. Y. Wang, Y. J. Wang, Y. B. Xu, Z. D. Zhang, and S. J. Pennycook, Science, **348**, 547 (2015).

[22] A. K. Yadav, C. T. Nelson, S. L. Hsu, Z. Hong, J. D. Clarkson, C. M. Schlepüetz, A. R. Damodaran, P. Shafer, E. Arenholz, L. R. Dedon, D. Chen, A. Vishwanath, A. M. Minor, L. Q. Chen, J. F. Scott, L. W. Martin and R. Ramesh, Nature, **530**, 198 (2016)
[23] R. G. P. McQuaid, A. Gruverman, J.F. Scott and J.M. Gregg, Nano Lett., **14**, 4230 (2014).
[24] N. Balke, B. Winchester, W. Ren, Y. H. Chu, A. N. Morozovska, E. A. Eliseev, M. Huijben, R. K. Vasudevan, P. Maksymovych, J. Britson, S. Jesse, I. Kornev, R. Ramesh, L. Bellaiche, L. Q. Chen and S. V. Kalinin, Nature Physics, **8**, 81 (2012).
[25] B. Matthias and A. von Hippel, Phys. Rev. **73**, 1378 (1948).
[26] H. Sato, E. Nakamura and H. Motegi, J. Phys. Soc. Jpn., **43**, 1811 (1977).
[27] K. Deguchi and E. Nakamura, J. Phys. Soc. Jpn., **30**, 301 (1971).
[28] E. Nakamura, H. Sato and H. Motegi, J. Phys. Soc. Jpn., **47**, 1567 (1979).
[29] M. Lambert, A. M. Quittet, C. Taupin and A. Guinier, Journal de Physique, **25**, 345 (1964).
[30] A. M. Glazer, J. G. Lewis and W. Kaminsky, Proc. Roy. Soc. A, **452**, 2751 (1996).
[31] X. Marti, P. Ferrer, J. Herrero-Albillos, J. Narvaez, V. Holy, N. Barrett, M. Alexe, and G. Catalan, Phys. Rev. Lett., **106**, 236101 (2011).
[32] N. Domingo, N. Bagues, J. Santiso and G. Catalan, Phys. Rev. B., **91**, 094111 (2015).
[33] A. Schilling, R. M. Bowman, G. Catalan, J. F. Scott and J. M. Gregg, Nano Letters, **7**, 3787 (2007); A. Schilling, R. M. Bowman and J. M. Gregg, G. Catalan and J. F. Scott, Appl. Phys. Lett. **89**, 212902 (2006).
[34] A. Schilling, T. B. Adams, R. M. Bowman, J. M. Gregg, G. Catalan and J. F. Scott, Phys. Rev. B, **74**, 024115 (2006).
[35] L. J. McGilly, T. L. Burnett, A. Schilling, M. G. Cain and J. M. Gregg, Phys. Rev. B., **85**, 054113 (2012).
[36] P. Marton, I. Rychetsky and J. Hlinka, Phys. Rev. B, **81**, 144125 (2010).
[37] L. Dong, D. S. Stone and R. S. Lakes, Phil. Mag. Lett., **90**, 23 (2010).
[38] H. D. Megaw, *Proc. Royal Soc. A.*,**189**, 261 (1947).
[39] W. P. Mason, Phys. Rev. **74**, 1134 (1948).
[40] W. J. Merz, Phys. Rev. **77**, 52 (1950).
[41] D. Walker, A. M. Glazer, S. Gorfman, J. Baruchel, P. Pernot, R. T. Kluender, F. Masiello, C. DeVreugd and P. A. Thomas, Phys. Rev. B. (article associated with the present manuscript to be published alongside it).

Figures:

Figure 1: Examination of a flux-grown $BaTiO_3$ crystal, using the METRIPOL microscope, shows the spontaneous formation of the square-net pattern reported by Forsbergh [2], Matthias and von Hippel [25] and Lambert *et al.* [29]. On heating, the periodic array appears spontaneously at around 111ºC and disappears at the Curie temperature of approximately 120ºC (as determined from the collapse in birefringence). The images show the orientation ϕ (top panels) and $|\sin\delta|$ (bottom panels) distributions at three temperatures. The crystal thickness is of the order of 300μm.

Figure 2: Room-temperature lateral piezoresponse force microscopy (PFM) imaging of the surface of a region of a flux-grown $BaTiO_3$ crystal, in which the Forsbergh birefringence pattern is found (amplitude (a) and phase (b)) shows evidence for packets of domains. However, they are not regularly distributed and do not obviously correspond to the specific polyhedral shapes envisaged by Forsbergh [2]. For completeness, the inset shows the orientation of the cantilever axis and the arrows indicate the directions of sensitivity to in-plane polarization components. The crystal surface is $\{001\}_{pseudocubic}$.

Figure 3: As noted by Forsbergh [2], square-net birefringence patterns only occur where perpendicular sets of a-c ferroelastic stripe domains meet, as can be seen in (a). The a-c domain contrast is indicated by line features parallel to the $<100>_{pseudocubic\ (pc)}$ directions (highlighted by fine blue arrows) consistent with lines of intersection of $[101]_{pc}$ and $[011]_{pc}$ a-c ferroelastic domain walls with the $(001)_{pc}$ $BaTiO_3$ surface. $\{110\}_{pc}$ a_1-a_2 domain walls would show stripe contrast features parallel to $<110>_{pc}$ directions on the same $(001)_{pc}$ surface and so can be discounted as responsible for the contrast. Where the perpendicular sets of lines meet, a square feature in birefringence can be seen. This transmission optical image was taken approximately 2^{o}C below T_C (crystal temperature estimated as 118^{o}C) under crossed polars using a white light source. Rather than consider hypothetical structures resulting from the impingement of a-c domain packets as responsible for the Forsbergh birefringence, an alternative microstructure was considered theoretically, in which two slabs (labelled slab 1 and slab 2) of perpendicularly oriented a-c domains are simply superposed (b). In this schematic, the orientation of polarization within each domain in the slabs is indicated by the coarse squat blue arrows.

Figure 4: The optical retardation (Δ) through each slab of a-c stripe domains will start to show spatial modulation when the ratio of domain periodicity (ω) to slab thickness (d) is

greater than or equal to $\sqrt{2}/_2$. The amplitude of the optical retardation will locally reach a maximum when $\omega/_d \geq \sqrt{2}$. The case where $\omega/_d = \sqrt{2}$ is considered schematically in (a) with a cross-section of the a-c stripe domains within a single slab (top panel) and the corresponding relative optical retardation (Δ/Δ_{max}) variation as a function of the ratio of distance, *x*, divided by domain period, ω (bottom panel in (a)). When two such slabs of a-c domains are placed one above the other, and at 90° to each other, the spatial variation in retardation is such that the Forsbergh pattern is reproduced, when viewed from above (b). Here, dark blue corresponds to the minimum relative retardation (0) and dark red to the maximum relative retardation (1) as indicated in the colour scale. Even if the slabs are not of equal thickness, square-net birefringence still occurs: as an illustration, in (c) the thickness of one slab is kept the same as that considered in (a), but the thickness of the second slab is increased by a factor of 1.5.

Figure 5: Scanning transmission electron microscopy (STEM) image of a single crystal $BaTiO_3$ pillar (beam parallel to a $<100>_{pc}$ direction), similar to those published by Schilling *et al.* in [33] and fabricated by Focused Ion Beam (FIB) patterning in the same manner as described in [33] (a); the image illustrates the way in which ferroelastic domain periodicity depends on the local dimensions of the domain packet containing the stripe domains: note how the domain periodicity decreases as the packet dimensions become progressively more constrained towards the points of the triangles in individual domain packets. For this image, the local domain period (ω) has been examined as a function of the local domain packet width (d) and the Landau-Kittel scaling relationship was found to hold reasonably well (b). By considering the way in which $\omega/_d$ varies with temperature, using equation (6) and literature values for Young's Modulus, spontaneous strain and domain wall energy (c), it can be seen that the ω/d ratio in slabs of a-c stripe domains only exceeds the two critical values of $\sqrt{2}/_2$ and $\sqrt{2}$ in a narrow region just below T_c. The width of this region grows as the slab thickness decreases, however it is much narrower than that observed experimentally in figure 1, for example. Recalculating the expected ω/d values using measurements by Walker *et al.* in [41] for the specific crystals studied herein (d), shows that the sudden collapse in spontaneous strain evident from X-ray diffraction causes a dramatic increase in the window of stability of the Forsbergh patterns (visible when the ω/d ratio exceeds $\sqrt{2}/_2$).

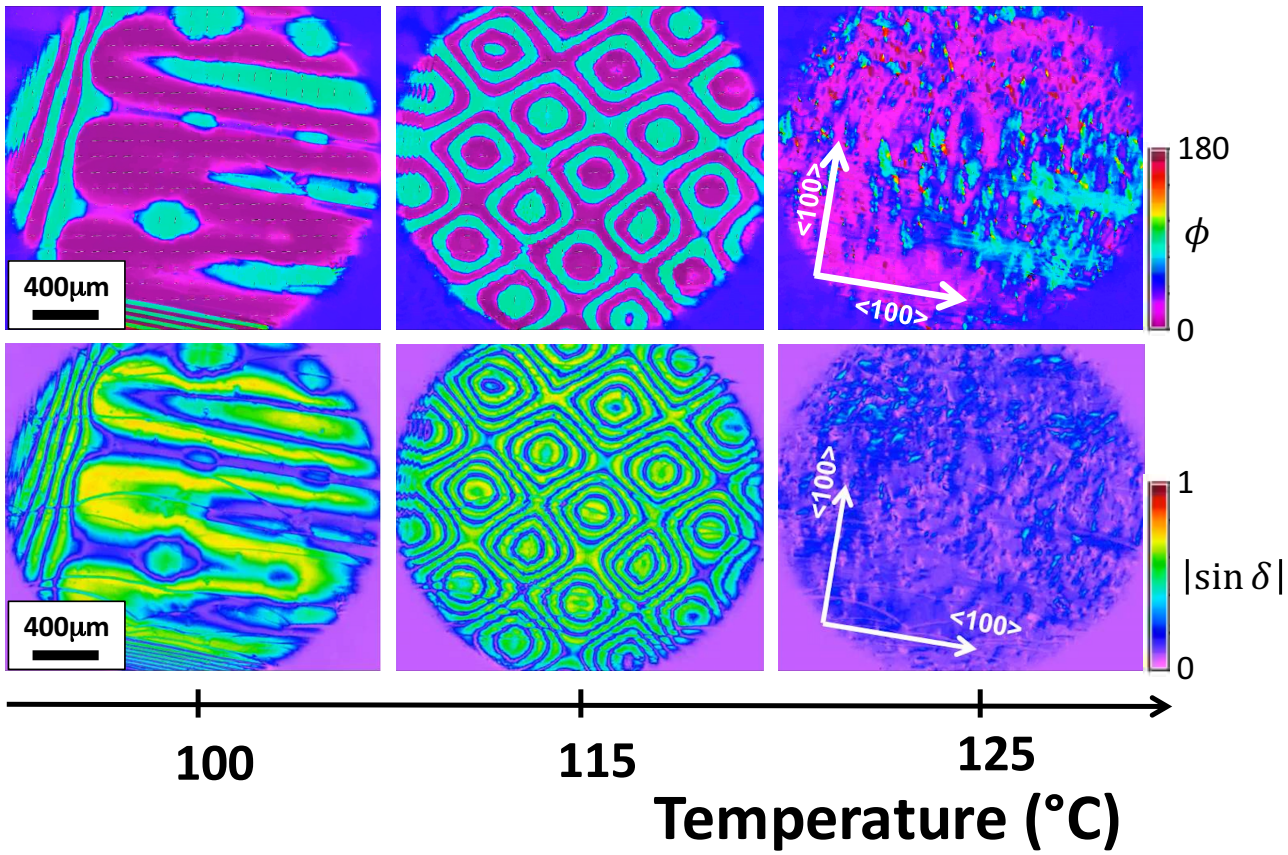

Figure 1 of 5: Schilling *et al.*

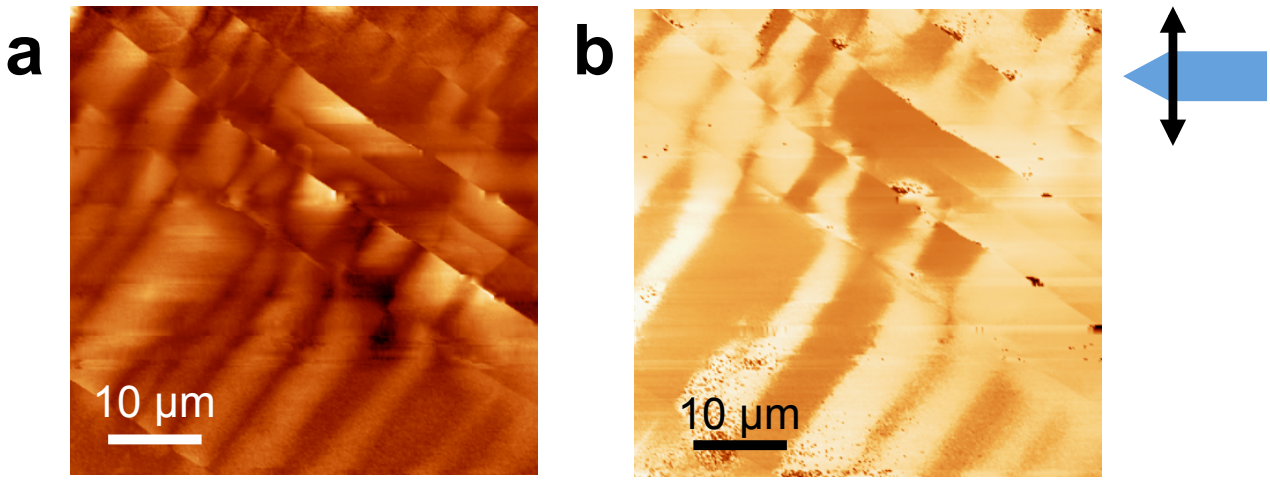

Figure 2 of 5: Schilling *et al.*

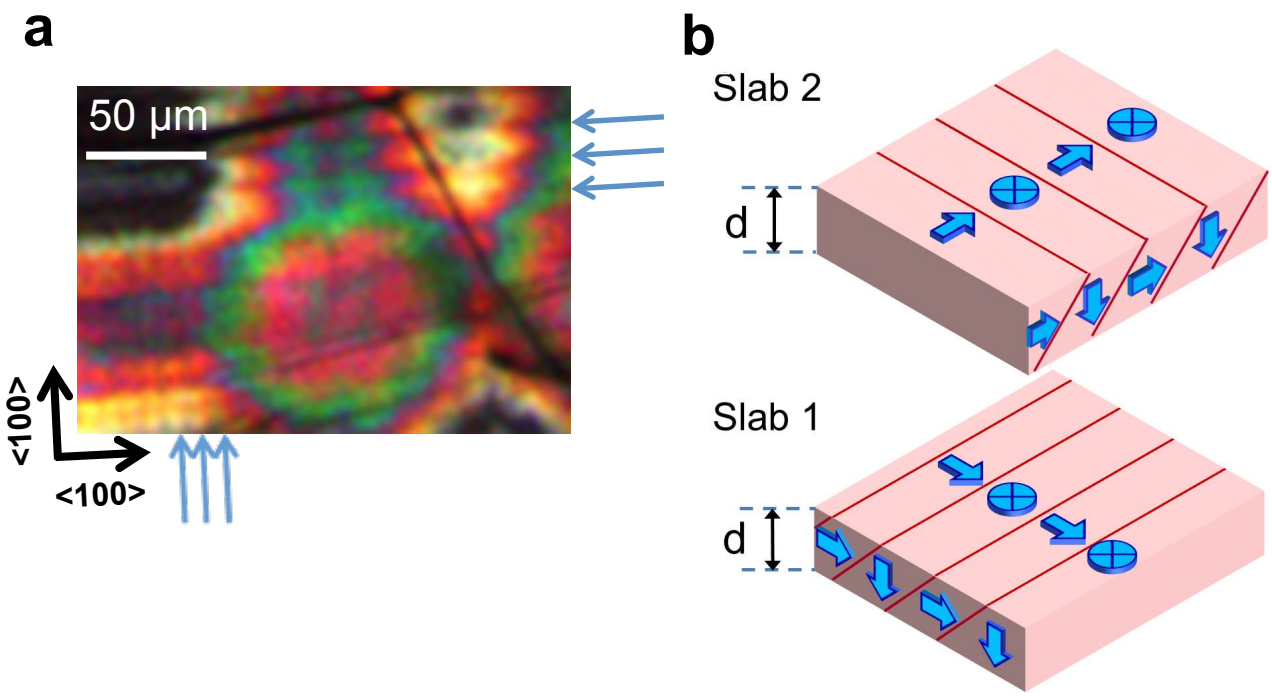

Figure 3 of 5: Schilling *et al.*

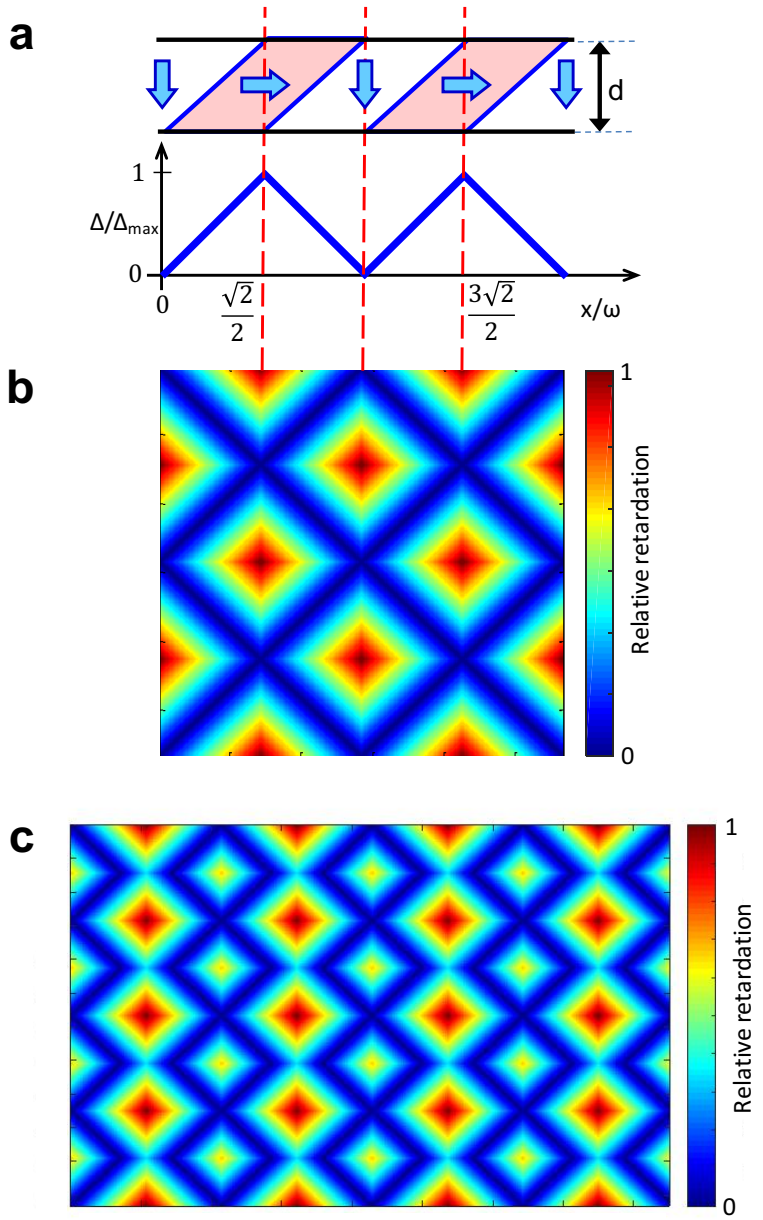

Figure 4 of 5: Schilling *et al.*

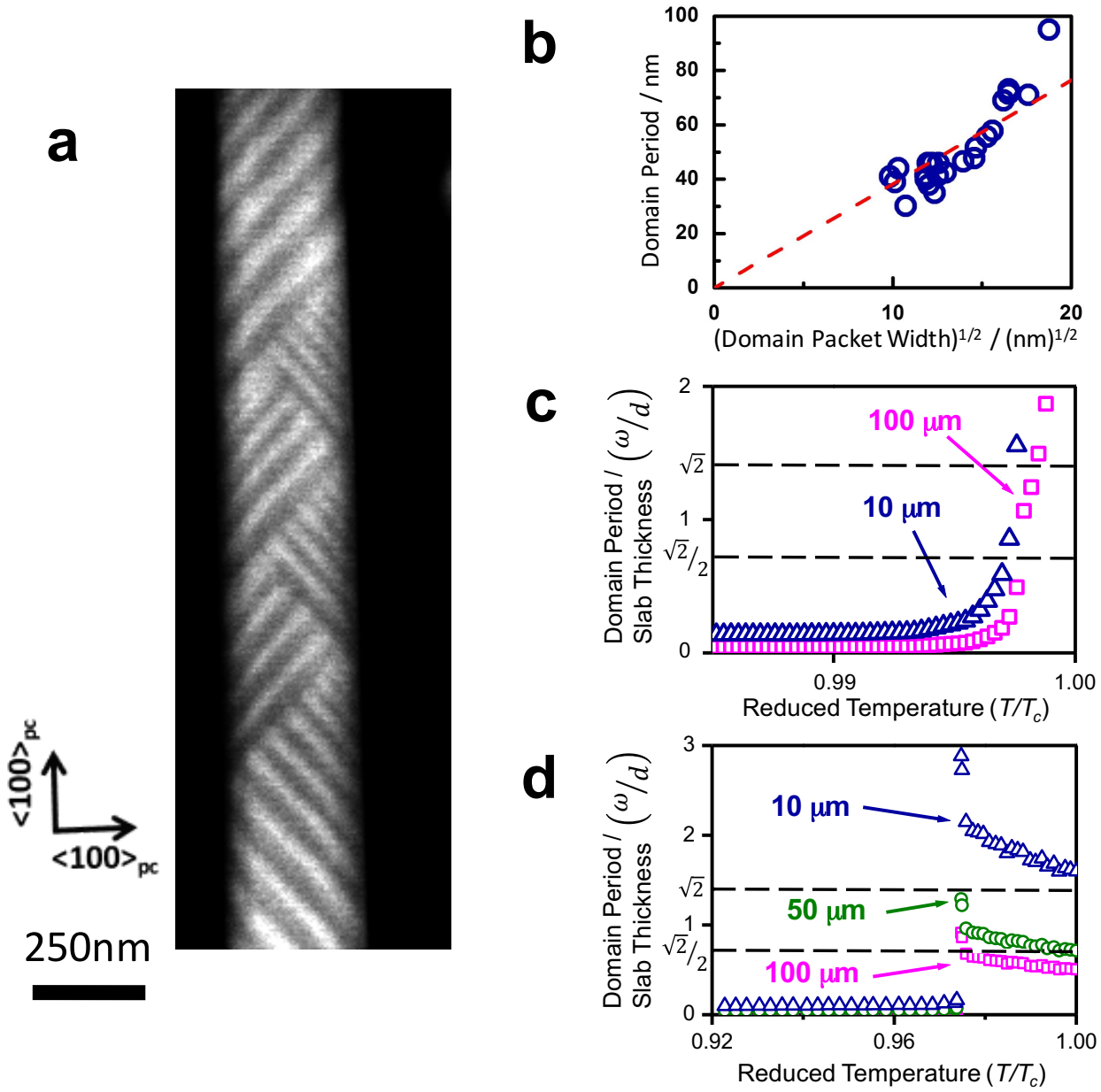

Figure 5 of 5: Schilling *et al.*